Building Research & Information

ISSN: 0961-3218 (Print) 1466-4321 (Online) Journal homepage: www.tandfonline.com/journals/rbri20

The effect of building typology and visual complexity on stress levels through amplitude spectrum analysis

Mirna Zordan, Petrus Jacobus Hermanus Maree, Zixian Lei, Tianze Xie & Seungwoo Je

To cite this article: Mirna Zordan, Petrus Jacobus Hermanus Maree, Zixian Lei, Tianze Xie & Seungwoo Je (09 Jul 2026): The effect of building typology and visual complexity on stress levels through amplitude spectrum analysis, Building Research & Information, DOI: 10.1080/09613218.2026.2691250

To link to this article: https://doi.org/10.1080/09613218.2026.2691250

Published online: 09 Jul 2026.

BUILDING RESEARCH & INFORMATION
https://doi.org/10.1080/09613218.2026.2691250

RESEARCH ARTICLE

The effect of building typology and visual complexity on stress levels through amplitude spectrum analysis

Mirna Zordan, Petrus Jacobus Hermanus Maree, Zixian Lei, Tianze Xie and Seungwoo Je

School of Design, Southern University of Science and Technology, Nanshan, People's Republic of China

ABSTRACT

Building typology shapes the visual structure of streetscapes and may influence stress-related physiological responses. This study develops a novel integrative framework that combines amplitude spectrum slope (-α) analysis, immersive Virtual Reality (VR), and Heart Rate Variability (HRV), indexed by the standard deviation of normal-to-normal intervals (SDNN), to examine how scene-level Spatial Frequency (SF) structure relates to physiological stress. Immersive 360° VR streetscape scenes were reconstructed for three representative Hong Kong building typologies, namely the cantilevered building typology, the super high-rise podium-tower typology, and the podium-tower typology. Amplitude spectrum slopes were calculated from video frames, and physiological stress responses were assessed using SDNN during three 5-minute exposure periods. The results showed significant differences in both α values and SDNN across the three typologies. The podium-tower typology exhibited the lowest mean α value (1.1758) and the highest mean SDNN (54.39), indicating comparatively lower physiological stress. Notably, this typology also produced the α value closest to 1, an SF pattern more consistent with the statistical regularity commonly observed in natural scenes. These findings highlight the potential of the proposed framework as a novel approach to inform evidence-based design in high-density urban environments.

ARTICLE HISTORY
Received 1 September 2025
Accepted 15 June 2026

KEYWORDS
Building typology; streetscapes; physiological stress; amplitude spectrum slope; heart rate variability; virtual reality

Introduction

Over the past several decades, urban areas have undergone extensive expansion, with high-density zones emerging as the predominant form of habitation. Such environments are typified by sky exposure, pronounced visual enclosure from surrounding built forms, and elevated levels of crowding at the neighbourhood scale (Asgarzadeh et al., 2014; Baum & Weiss, 1987; Hartig et al., 2014). These characteristics collectively exacerbate individual stress, the chronic accumulation of which is linked to an increased incidence of mental health disorders and a consequent decline in quality of life (Liu et al., 2015). Accordingly, it is imperative to identify and evaluate the factors that modulate stress responses within high-density contexts.

Among these factors, building typology critically shapes both the perceptual and physiological experiences of outdoor environments (Lenzholzer & de Vries, 2020; St-Jean et al., 2022). Although certain typologies have been associated with enhanced satisfaction and preference, the specific contributions of typological attributes such as configuration, composition, and spatial arrangement remain underexplored, particularly in relation to stress.

Building typology directly informs visual complexity, a key perceptual attribute defined by the amount of information and level of detail present in a scene (Oliva et al., 2004; Snodgrass & Vanderwart, 1980). Visual complexity arises from the interplay of typology, morphological features, and human activity (Baum & Weiss, 1987), and profoundly influences physiological markers of arousal, such as heart rate and skin conductance (Harper et al., 2009; Tuch et al., 2009). Spatial Frequency (SF) characteristics, quantified via the amplitude spectrum slope (-α), offer a robust metric for assessing visual complexity in architectural imagery (Isherwood et al., 2017). By calculating α values for different building typologies, researchers can elucidate how variations in building form influence environmental perception and stress-related physiological responses through the lens of visual complexity.

The amplitude spectrum slope provides a quantitative measure of the SF composition of an image, reflecting how signal intensity decays with increasing frequency in $1/f^{\alpha}$ noise (Spehar et al., 2015). In natural scenes, α typically approximates 1, and deviations from this value have been associated with visual discomfort and stress

CONTACT Mirna Zordan mzordan@sustech.edu.cn

(Field, 1987; Juricevic et al., 2010; Penacchio & Wilkins, 2015). Through Fourier transformation, streetscape images can be translated into spectral representations, from which the amplitude spectrum slope can be derived. Earlier streetscape studies by Seta and colleagues made related attempts to evaluate urban scenes using fluctuation theory and Fourier-based descriptors (Seta et al., 2002, 2003). These findings suggest that amplitude spectrum slope is a relevant descriptor of visual structure in built environments and a potential basis for examining stress-related responses.

Building on this line of work, this study introduces a novel hybrid framework that integrates Fourier-based amplitude spectrum analysis ($1/f^{\alpha}$) with HRV-based physiological stress in immersive VR environments. Utilizing three representative Hong Kong block typologies, this study investigates how variations in building typology influence spectral image properties and their subsequent impact on human stress responses.

Conceptual background and related work

Building typology and human perception

Previous research has shown that architectural and environmental configurations shape human perception, comfort, anticipatory experience, and stress responses across built settings (Evans et al., 2003; Matsumoto & Seta, 1999; Persiani et al., 2021; Ulrich, 1991). In outdoor environments, these effects are especially evident at the neighbourhood and streetscape scales, where building morphology influences how people experience enclosure, legibility, comfort, and emotional response (Liang et al., 2024; Liu et al., 2015). Building typology is therefore not merely a physical description of urban form, but also an important factor in shaping how outdoor built environments are perceived and experienced.

Among the attributes through which building typology may influence these responses are enclosure, sky exposure, façade articulation, and overall spatial composition (Boubekri et al., 2014; Gao et al., 2025; Liang et al., 2024). Previous studies have shown that reduced sky exposure and highly enclosed urban conditions can intensify oppressive experiences, whereas more open and visually accessible environments are often associated with improved mood, relaxation, and stress recovery (Asgarzadeh et al., 2014; Boubekri et al., 2014; Gao et al., 2025; Kozaki et al., 2012; Xiang et al., 2021). In addition, some studies suggest that façade articulation and visual complexity contribute to streetscape appraisal, while broader spatial composition may also influence affective evaluation and perceived restorativeness (Buttazzoni & Minaker, 2023; Hashemi Kashani et al., 2023; Liang et al., 2024). Collectively, these findings suggest that building typology and its associated morphological attributes play an important role in shaping human responses to outdoor built environments.

Visual complexity

Visual complexity constitutes a fundamental dimension of perceptual quality and is closely associated with affective evaluations of the environment (Cavalcante et al., 2014). It influences pedestrian preferences (Ewing, 2013; Kaplan et al., 1972), relates to perceptions of safety and comfort in outdoor settings (Hartig et al., 2014), and has been associated with physiological responses during visual experience of environments (Tuch et al., 2009). In architectural and urban contexts, visual complexity also varies with the observer's distance from built elements and contributes to the way environments are experienced and interpreted (Ma et al., 2020; Zordan & Je, 2024). Taken together, these findings position visual complexity as an important perceptual factor through which characteristics of the built environment may influence human experience and stress-related responses.

Visual complexity has been associated with various quantitative indicators, such as fractals (Jacquin, 1992), information entropy (Rigau et al., 2005), and SF (Isherwood et al., 2017). Seta et al. (2002, 2003) examined disorder, regularity, and attraction in urban scenes by linking streetscape elements with quantitative descriptors derived from fluctuation theory and Fourier analysis. Cavalcante et al. (2014) further demonstrated that streetscape complexity can be characterized using local contrast statistics and SF-related properties. Building on this line of research, the present study treats visual complexity as a scene-level property reflected in SF structure.

Spatial frequency and $1/f^{\alpha}$ noise

Spatial Frequency (SF) characteristics play a central role in visual perception because they describe how image information is distributed across different scales. High spatial frequencies correspond to fine details such as edges, contours, and textures, whereas low spatial frequencies represent broader luminance variations and larger structural forms (Campbell & Robson, 1968; Ellemberg et al., 2012; Ginsburg, 1971, 1986). Because visual scenes are composed of information at multiple scales, SF analysis provides a useful framework for characterizing the overall visual structure of built environments.

In image analysis, SF is commonly quantified through the spectral slope, or $1/f^{\alpha}$ relationship, which describes how image amplitude decays as frequency increases (Bex & Makous, 2002; Celikors & Wells, 2022). The relationship can be expressed as:

$$A(f) \propto f^{-\alpha} \tag{1}$$

where $A(f)$ represents the amplitude at SF f, and α is the exponent governing the rate at which the amplitude decreases as frequency increases. On a log–log scale, this relationship corresponds to a slope of $-\alpha$ (Bex & Makous, 2002). The amplitude spectra of many natural scenes approximate this power-law form, and images with α values close to 1 are often considered statistically similar to natural-scene structure (Field, 1987; Penacchio & Wilkins, 2015).

The relevance of this measure is further supported by evidence linking amplitude spectrum characteristics to visual comfort. Prior studies have shown that images whose spectral slopes are closer to those commonly found in natural scenes are generally processed more fluently and are associated with lower visual discomfort, whereas deviations from this range may induce discomfort and stress (Field, 1987; Juricevic et al., 2010; Penacchio & Wilkins, 2015; Spehar et al., 2015; Wilkins, 2016). Consistent with this view, images with spectral slopes closer to those of natural scenes are generally perceived as more visually comfortable than images with steeper or flatter slopes (Fernandez & Wilkins, 2008; Juricevic et al., 2010; Wilkins, 2016). Extending earlier Fourier-based approaches to streetscape evaluation, the present study uses amplitude spectrum slope as a scalar descriptor of scene-level SF structure to examine whether building typologies differ in their spectral profiles and whether these differences are associated with physiological stress responses.

Heart rate variability as an indicator of physiological stress

Heart Rate Variability (HRV) refers to the variation in successive heartbeat intervals and is widely regarded as a non-invasive indicator of autonomic nervous system function (Acharya et al., 2006; Barbieri et al., 2005; Thayer et al., 2010). Because it reflects the heart's capacity to adapt to physiological and environmental demands, HRV has been extensively used to assess stress-related physiological responses in a continuous and objective manner (Kim et al., 2018; Vigo et al., 2019). This makes HRV particularly suitable for examining how different built-environment conditions may influence human stress.

Among HRV indices, the Standard Deviation of Normal-to-Normal intervals (SDNN) is one of the most commonly used time-domain measures of overall autonomic variability and has been widely applied in stress research (Acharya et al., 2006; Kim et al., 2018; Yeom et al., 2021). Lower SDNN values generally indicate reduced autonomic flexibility and higher physiological stress, whereas higher values suggest greater adaptive capacity and recovery potential (Gaertner et al., 2023; Kim et al., 2018). Accordingly, the present study uses SDNN as the principal physiological indicator for evaluating stress responses across different building typologies.

Objectives of the present research

Although numerous studies have shown that the built environment influences individuals' environmental perception, fewer have examined how different building typologies shape SF characteristics of the streetscapes and how these characteristics relate to physiological stress. This study, therefore, investigates whether different building typologies are associated with different amplitude spectrum slopes and whether such differences are reflected in HRV-based stress responses. In this way, the study develops a novel integrative framework for examining the relationship between streetscape visual structure and human stress.

Methods

Overview of research design

This study examines whether different building typologies are associated with differences in scene-level SF structure and physiological stress responses. As shown in Figure 1, the research combines image-based amplitude spectrum slope analysis with an immersive VR experiment and HRV measurement. Panoramic street scenes representing three Hong Kong building typologies were recorded, transferred into VR simulations, and analysed in relation to participants' SDNN responses.

Environmental stimuli and design

Hong Kong provides a relevant context for this study because its compact, high-rise, and high-density urban form has generated several distinct building typologies in response to land scarcity and development pressure (Lau, 2011; Lau & Zhang, 2015). Against this background, the study focuses on three representative typologies: the cantilevered building typology, the podium-tower, and the super high-rise podium-tower (Lau & Zhang, 2015) (see Figure 2). These typologies exemplify different architectural responses to urban density and land scarcity, and are characterized by distinct morphological features relevant to streetscape perception and visual analysis.

Typology A: cantilevered building typology

Prevalent in the 1950s and 1960s, this typology is characterized by cantilevered buildings extending over public areas (Lau & Zhang, 2015). Typology A, exemplified by

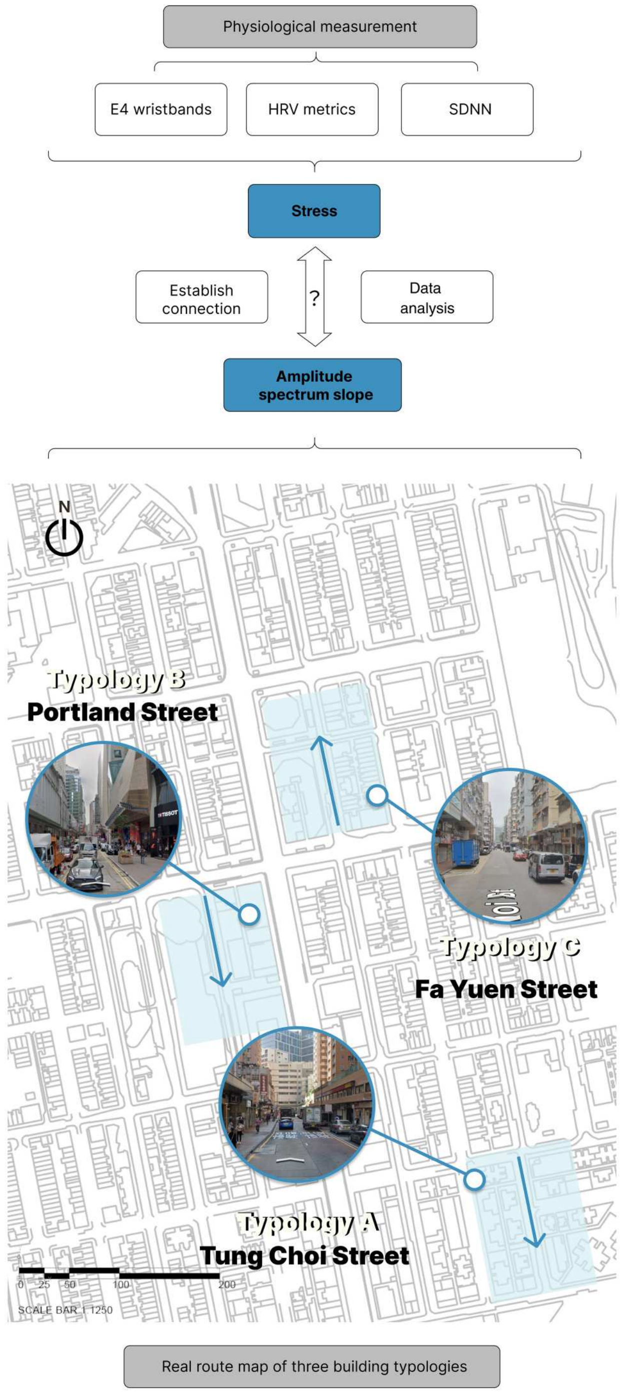

Figure 1. The framework of the present study. The image below is a keymap of the recorded video materials used in this study, illustrating the routes shown in the video.

buildings along Tung Choi Street in Kowloon, Hong Kong, features dense commercial uses on the lower floors and residential units above. The distinctive feature of these buildings is the setback at the first-floor level.

Typology B: super high-rise podium-tower typology

Emerging after 2000, this typology remains widely adopted, distinguished by an expanded podium volume and tower heights exceeding 40 floors, culminating in super high-rise podium-tower configurations (Lau & Zhang, 2015). Typology B, located on Portland Street in Kowloon (notably Langham Place), primarily comprises super high-rise podium-towers. This typology is featured by a linear street frontage and a monolithic appearance, exhibiting minimal fragmentation at both ground and facade levels. It predominantly incorporates glass curtain walls that function as merchandise displays.

Typology C: podium-tower typology

Emerging in the 1980s, this typology exemplifies Hong Kong's mixed land-use model by vertically separating residential and commercial functions (Lau & Zhang, 2015). Typology C, represented by buildings along Fa Yuen Street in Kowloon, consists of a lower podium supporting an upper tower. The typology extends linearly, with the ground floor marked by significant fragmentation due to numerous commercial tenants. The podium is articulated at a pedestrian scale, emphasizing a high degree of transparency at street level.

On-site data collection and image processing

The VR stimuli comprised three distinct immersive street experiences, each recreated through separate 360° videos that showcased one of Hong Kong's selected building typologies and corresponding streetscapes: Tung Choi Street, Portland Street, and Fa Yuen Street. The videos were recorded using an INSTA360 X3 panoramic camera at a resolution of 5760×2880 pixels and a frame rate of 30 frames per second. Filming took place under overcast conditions, with an average temperature of 24.4°C and approximately 79% cloud cover, which helped minimize pedestrian traffic and distractions.

The 360° videos were deconstructed into individual frames at 30 frames per second, yielding a total of 27,000 images (9,000 frames per building typology). To standardize the visual input for amplitude spectrum slope analysis, batch-processing scripts were used to crop each frame using a fixed vertical field-of-view threshold of ±45°, as illustrated in Figure 3.

Amplitude spectrum slope analysis

Images representing the three building typologies were processed to estimate the amplitude spectrum slope ($-\alpha$) from their SF distributions. Each image was converted from the spatial domain to the frequency domain using a Two-Dimensional Discrete Fourier Transform (2D-DFT), as illustrated in Figure 4.

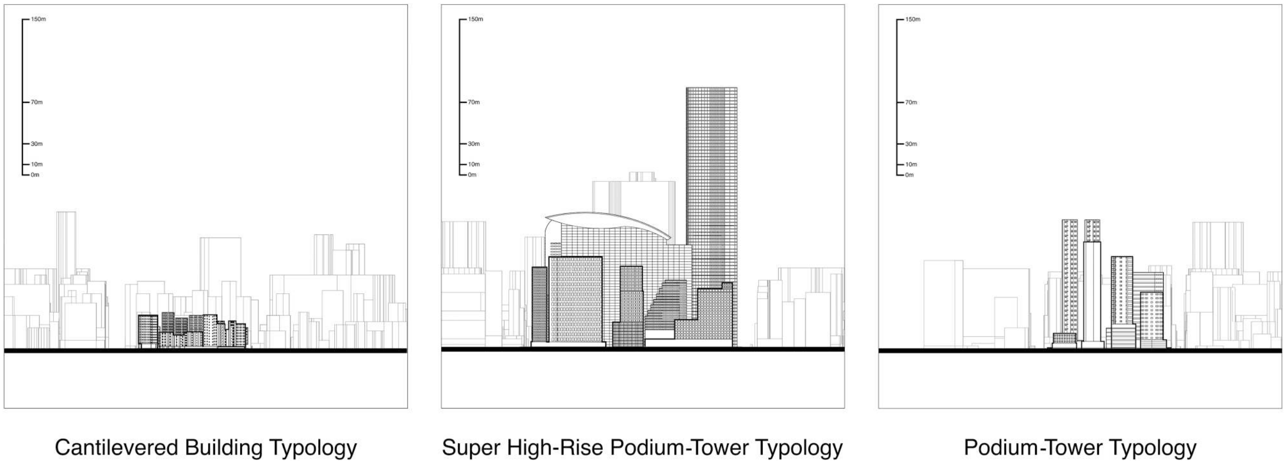

Figure 2. Three building typologies: the cantilevered building typology, located on Tung Choi Street, features cantilevered buildings extending over public areas; the super high-rise podium-tower typology, located on Portland Street, is distinguished by tower heights exceeding 40 floors; and the podium-tower typology, located on Fa Yuen Street, is characterized by a vertical separation between residential and commercial spaces.

Initially, the images were converted to greyscale by averaging the colour channels. The pre-processed image $I(x, y)$of size $M \times N$ was then transformed into the frequency domain using a two-dimensional discrete Fourier transform (2D-DFT), as expressed in Equation (2):

$$F(u, v) = \sum_{x=0}^{M-1} \sum_{y=0}^{N-1} I(x, y) e^{-i2\pi\left(\frac{ux}{M} + \frac{vy}{N}\right)},$$

where $u \in [0, M-1]$ and $v \in [0, N-1]$ denote the frequency indices. The zero-frequency component was shifted to the centre of the spectrum using the operation $F_{\text{shifted}}(u, v) = \text{FFTShift}(F(u, v))$.

Subsequently, the amplitude spectrum $A(u, v)$ was computed as the magnitude of the Fourier coefficients, defined by Equation (3):

$$A(u, v) = |F_{shifted}(u, v)|. \quad (3)$$

To mitigate the influence of image aspect ratio on the frequency scale, the calculation of the radial frequency r_k incorporates normalization by the visual angle

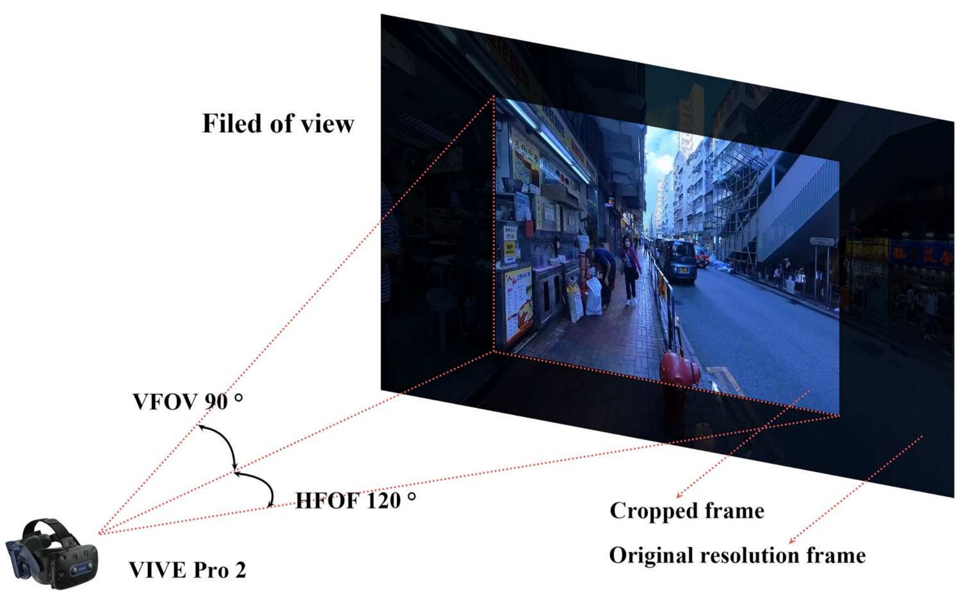

Figure 3. Field of View (FOV) during the participant's experiment: VFOV refers to Vertical Field of View; HFOV refers to Horizontal Field of View.

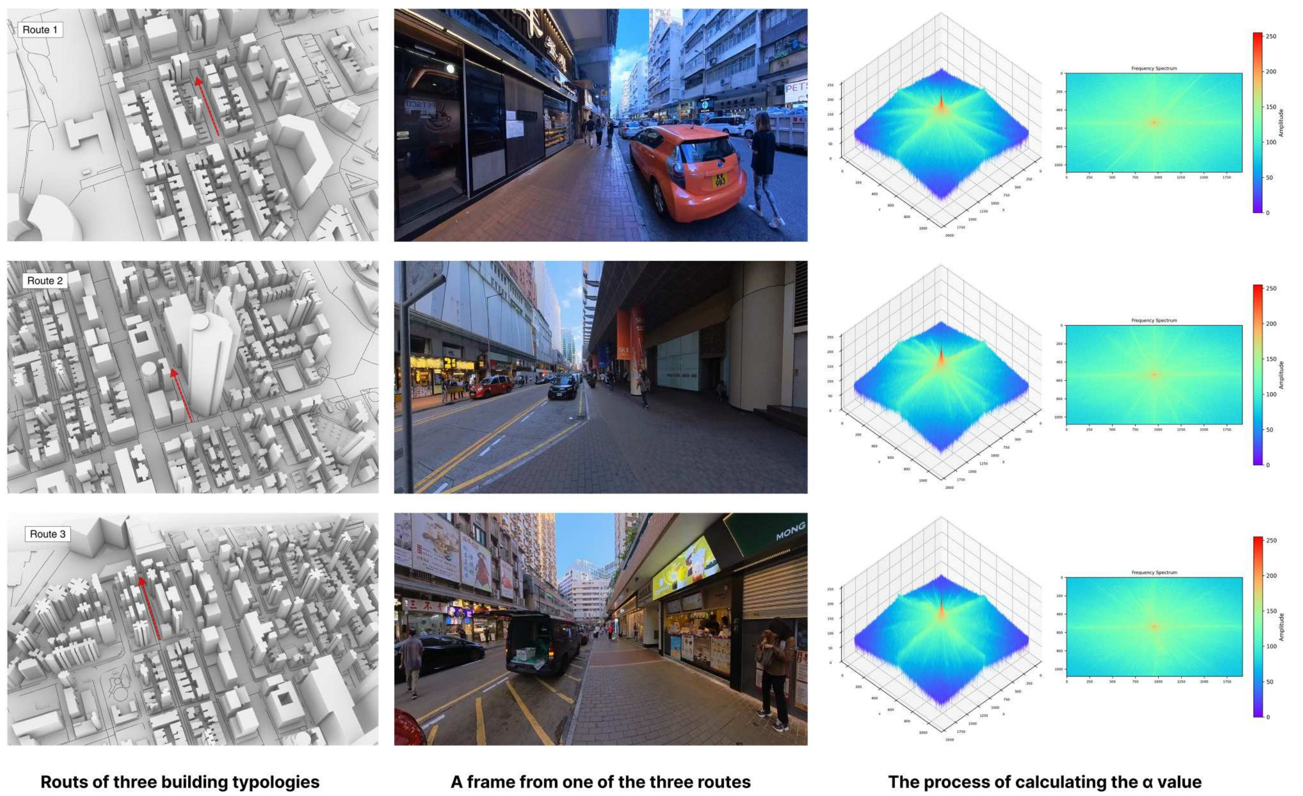

Figure 4. Visualization of spatial domain conversion to frequency domain.

resolution, as defined in Equation (4).

$$r_k = \sqrt{\left(\frac{u - M/2}{M} \cdot \theta_x\right)^2 + \left(\frac{v - N/2}{N} \cdot \theta_y\right)^2}, \qquad (4)$$

where $\theta_x = 120°$ represents the horizontal field of view, and $\theta_y = \theta_x \cdot (N/M)$ denotes the vertical field of view, thereby ensuring frequency units in cycles per degree (CPD).

The amplitude spectrum was then partitioned into logarithmically spaced frequency bins. The mean amplitude $\bar{A}(k)$ within each bin k was calculated as follows (Equation 5):

$$\bar{A}(k) = \frac{1}{N_k} \sum_{r(u,v) \in bin_k} A(u, v), \qquad (5)$$

where N_k denotes the number of frequency points within bin k. Logarithmic binning was employed to accommodate the exponential decay of amplitude with increasing frequency.

The mean amplitude values $\bar{A}(k)$ and their corresponding bin centre frequencies r_k were transformed to logarithmic scales. A linear regression model was fitted over the frequency range of 0.06–1 cycle per degree (CPD) (Equation 6):

$$\log \bar{A}(k) = -\alpha \cdot \log r_k + c + \epsilon_k, \qquad (6)$$

where $-\alpha$ represents the amplitude spectrum slope, c is the intercept, and ϵ_k denotes residuals. The slope α was estimated via least squares minimization (Equation 7):

$$\alpha = -\frac{\sum_{k=1}^{N} \left(\log r_k - \overline{\log r}\right)\left(\log \bar{A}(k) - \overline{\log \bar{A}}\right)}{\sum_{k=1}^{N} \left(\log r_k - \overline{\log r}\right)^2}, \qquad (7)$$

where $\overline{\log r}$ and $\overline{\log \bar{A}}$ are the means.

All 27,000 images representing the building typologies were analysed following this procedure, as illustrated in Figure 5. The analysis was conducted on the preprocessed images described in Section 3.3. Frequency components outside the 0.06–1 CPD range were excluded to focus on perceptually salient scales.

VR experiment: data collection and statistical analysis

Participants

The required sample size was calculated using G*Power with an alpha level of 0.05, an effect size (f) of 0.25, a power of 0.80, and a correlation among repeated measures of r = 0.65 (de Groot et al., 2021; van Ast et al., 2022), resulting in a minimum of 20

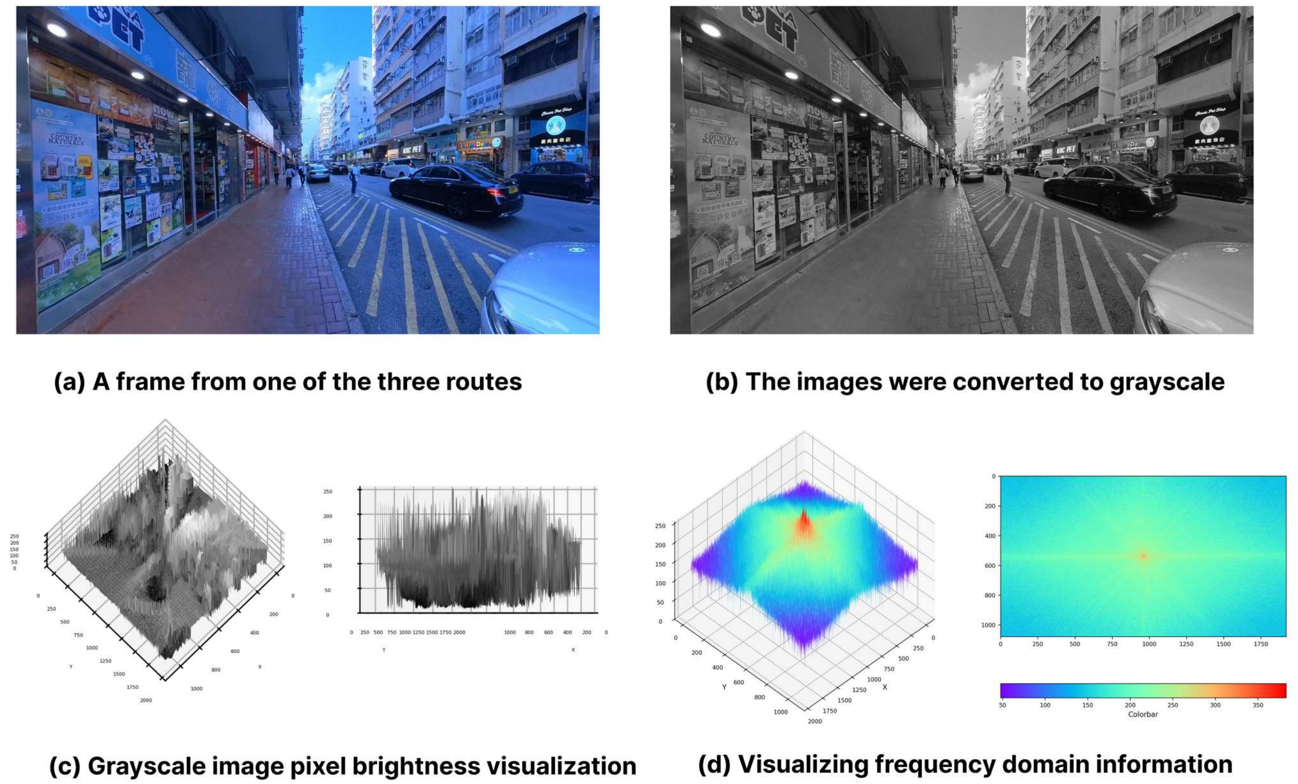

Figure 5. Visualization of amplitude spectrum slope calculation for Typology A: (a) original video frame as seen in the VR headset; (b) greyscale conversion of the frame; (c) pixel-brightness map of the greyscale image; (d) frequency-domain representation, with colour indicating amplitude of each SF component.

participants. A total of 27 participants aged 18–30 were recruited for the VR experiments through a combination of online and offline recruitment questionnaires. Data from 3 participants were excluded due to severe motion sickness, leaving 24 participants for the final analysis (Table 1).

To reduce the confounding effects of environmental familiarity, participants were required to be unfamiliar with the three experimental street scenes (Epstein et al., 2007; Scannell & Gifford, 2017). They were informed about the study procedure but were not told the specific building typologies represented in the stimuli. Exclusion criteria included individuals under 18 years of age, those with diagnosed psychological, neurological, or motor disorders, or any conditions potentially impairing normal functioning. Additionally, exclusion applied to participants currently taking mental health medications (e.g. for stress management), those prone to severe motion sickness, and individuals with visual or auditory impairments (including colour blindness), regardless of corrective device use (e.g. glasses, lenses, or hearing aids).

Table 1. Demographic characteristics of study participants.

Source	N = 24 Number	Rate (%)
Gender		
Male	10	41.67%
Female	14	58.33%
Age		
≤19	5	20.83%
19–20	3	12.50%
20–21	6	25.00%
21–22	5	20.83%
≥22	5	20.83%

Experiment procedure

This study comprises four main processes (S0, S1, S2, and S3), three intermission processes (T1, T2, and T3), and one additional process (A1), as depicted in Figure 6. The workflow of this study is illustrated in Figure 7. S0 represents the preliminary phase, which involves calibrating the equipment.

S1, S2, and S3 correspond to the three building typologies featured in the experiment: S1 showcases the cantilevered living quarters represented by Tung Choi Street. S2 presents the typology of a super high-rise podium-tower on Portland Street. S3 depicts the podium-tower typology on Fa Yuen Street. Each of these phases is divided into equal 5-minute intervals based on the length of the videos from the three experimental VR scenes. During the S1, S2, and S3 phases, heart rate data were collected to assess subjects'

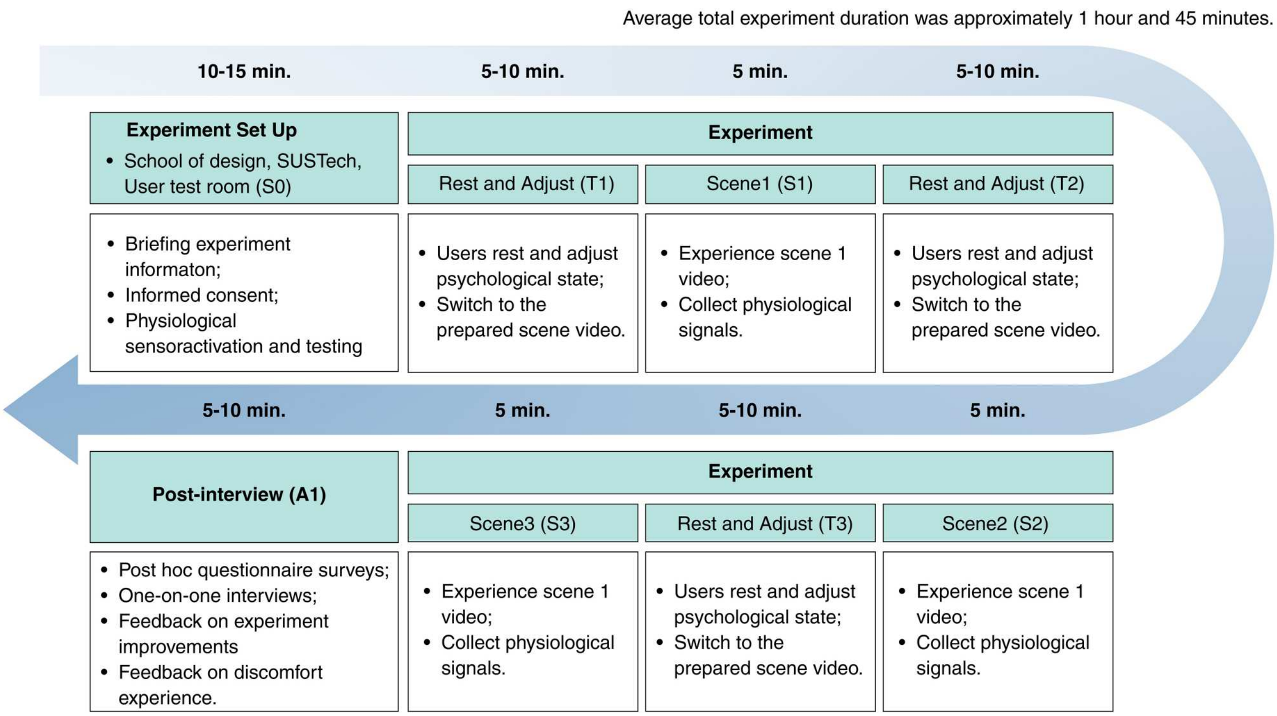

Figure 6. Experimental procedure.

physiological stress while exposed to different building typologies (Figure 6).

T1 is a brief intermission for equipment calibration and a quick screening check of the participants. T2 and T3 are intermission phases designed to facilitate transitions between the videos with recalibration of the equipment, if necessary.

In A1, participants were asked to evaluate their previous exposure to the virtual environments. They also reported symptoms such as general discomfort, fatigue, eye strain, and dizziness. In addition, one-on-one interviews and the collection of feedback from participants regarding potential improvements to the experiment were conducted.

An online questionnaire was administered five to seven days before the experiment to collect relevant background information. This study adhered to the World Medical Association Declaration of Helsinki and was approved by the Institutional Review Board of the affiliated institution. The experiment was conducted in a lab-controlled environment in December 2023.

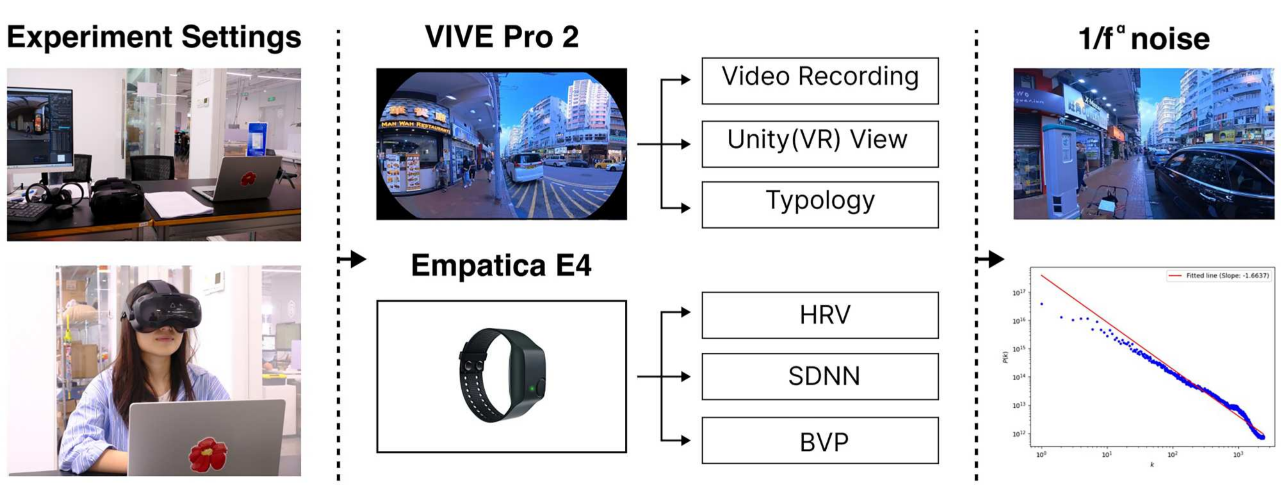

Figure 7. Workflow example: 360° video recordings of three street typologies were captured and processed frame by frame to calculate amplitude spectrum slope values. Simultaneously, participants immersed in these VR environments wore an Empatica E4 wristband to record physiological data, enabling analysis of the relationship between building typology and stress.

Physiological data collection and analysis

Physiological data were collected using the Empatica E4 wristband and its integrated sensors. The device was worn on the participants' left wrist, and RR interval data were collected using the wristband's Photoplethysmography (PPG) sensor, from which HRV metrics were derived. In the present study, SDNN was used as the principal physiological indicator of stress responses across the three building typologies.

HRV data were analysed for the three 5-minute exposure periods corresponding to the experimental typologies (see Figure 6). Kubios HRV Standard software was used to process the RR interval data and calculate SDNN values (Tarvainen et al., 2014). No pre-exposure baseline HRV measurement was recorded; therefore, the physiological analysis focused on relative differences in SDNN across the three typology-specific exposure conditions rather than baseline-adjusted changes.

Statistical analysis

Standard descriptive statistics were calculated for both amplitude spectrum slope ($-\alpha$) and SDNN across the three building typologies. For the image-based analysis, one-way ANOVA was used to assess differences in α values among the typologies, followed by Bonferroni post hoc pairwise comparisons. For the physiological data, a Friedman test was conducted to evaluate overall differences in SDNN across the three experimental conditions, followed by post hoc Wilcoxon signed-rank tests for pairwise comparisons. Comparative interpretation of α and SDNN was performed at the typology level. For each building typology, α values were computed frame by frame from the 9000 images extracted from the corresponding 5-minute VR video, whereas SDNN values were calculated for each participant during the corresponding 5-minute exposure period. Thus, the two measures were aligned at the condition level rather than through frame-level temporal matching.

Results

Amplitude spectrum slope (−a) results

The amplitude spectrum slope ($-\alpha$) was estimated for each frame image based on the log–log relationship between SF and amplitude. The resulting α values were used for subsequent analyses. Figures 8–10 illustrate the variation of α values across the frame sequences, and Figure 11 shows their overall distributions for the three building typologies. Descriptive statistics of α values are presented in Table 2, and inter-group differences were evaluated using one-way ANOVA.

The results in Table 2 indicate that the podium-tower typology (Typology C) exhibited the lowest average α value (1.1758). In contrast, the cantilevered building typology (Typology A) displayed a moderate average α value of 1.2037. The super high-rise podium-tower typology (Typology B) demonstrated the highest α value.

A one-way ANOVA was conducted to assess inter-group differences in α values derived from images cropped using the standardized ±45° vertical field-of-view threshold. The results, presented in Tables 3 and 4 and Figure 12, demonstrate significant differences in α values among the three building typologies ($p < 0.05$ for all comparisons). These findings suggest that the three typologies exhibit distinct scene-level SF characteristics.

Physiological indicators of stress

Analysis of the SDNN data provided insights into variations in participants' physiological stress across the three building typologies (see Table 2). The Friedman test, followed by post hoc Wilcoxon signed-rank tests, revealed statistically significant differences among the conditions ($\chi^2 = 9.75$, $p = 0.008$). Specifically, the Wilcoxon signed-rank tests showed significant differences in physiological stress between Typology A and Typology C ($Z = -2.11$, $p = 0.034$) and between Typology B and Typology C ($Z = -2.77$, $p = 0.006$). However, no significant difference was found between Typology A and Typology B ($Z = -1.00$, $p = 0.317$). These results indicate relatively higher physiological stress in the environments of Typologies A and B compared to Typology C.

Typology-level comparison of amplitude spectrum slope and physiological stress

Table 5 summarizes the typology-level comparison of image-based and physiological indicators. Typology C showed the lowest mean α value (1.1758), associated with the highest SDNN value (54.39), indicating relatively lower physiological stress under the tested condition, whereas Typologies A and B showed lower SDNN values. Taken together, these results suggest that the typology with α closest to 1 was also associated with comparatively lower physiological stress. However, because α and SDNN were aligned at the condition level rather than through frame-level temporal matching, this result should be interpreted as a cross-condition association rather than a direct moment-to-moment correspondence.

Discussion

The results show that Typology C exhibited the α value closest to 1 and the highest SDNN, whereas Typologies

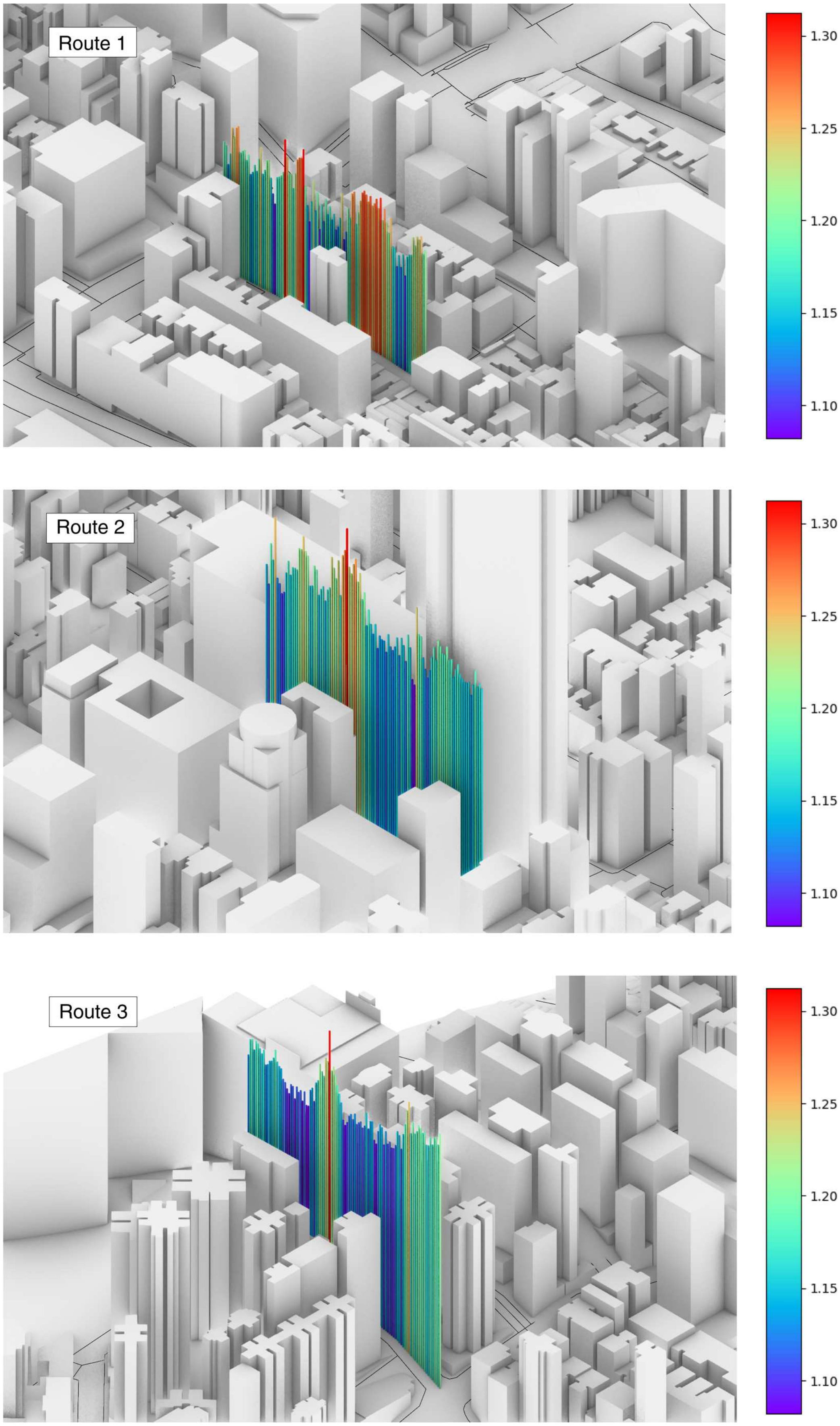

Figure 8. Visualization maps of α values of each frame image across the three street typologies.

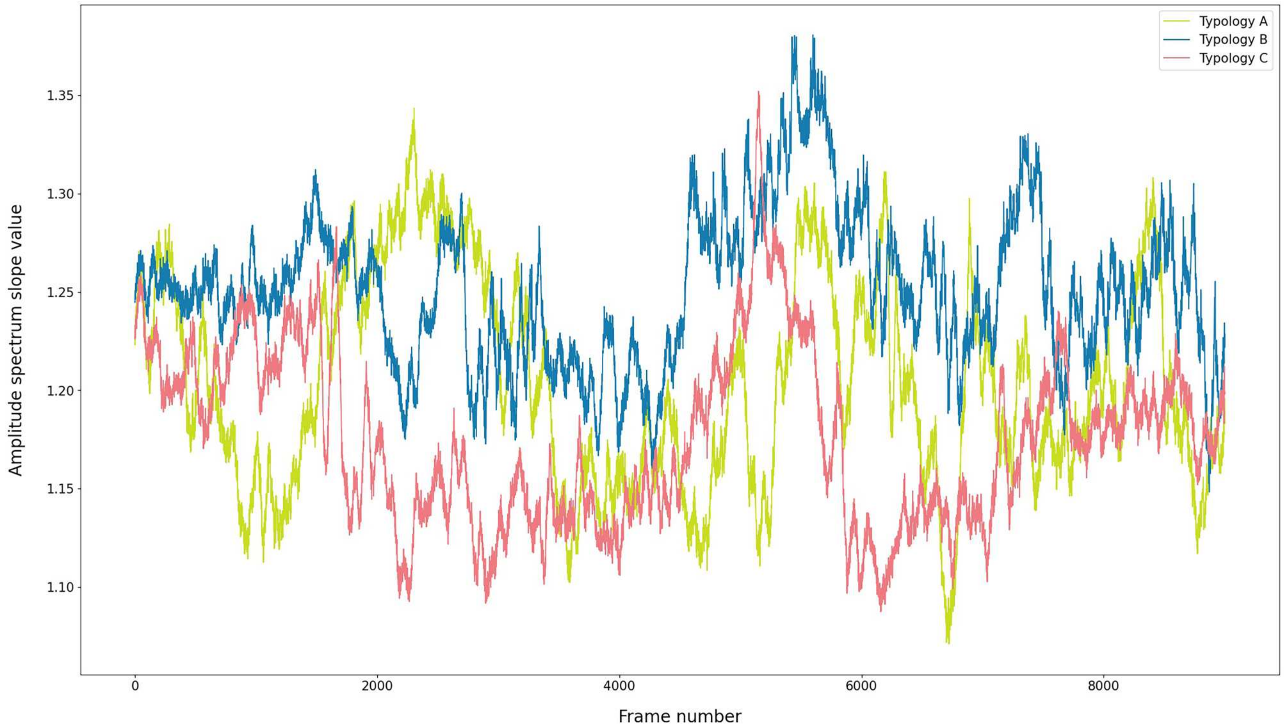

Figure 9. Variation of α values across the frame sequence for each of the three building typologies.

A and B were associated with higher α values and lower SDNN. The following discussion interprets these differences from a SF perspective and considers their implications for building typology and relative physiological stress.

Podium-tower typology: lower a value and lower relative physiological stress

The findings suggest that the podium-tower typology (Typology C) was associated with the lowest physiological stress among the three conditions, as indicated by the highest SDNN, and it also exhibited the α value closest to 1 (mean $\alpha = 1.1758$). In the present study, α is interpreted as a quantitative descriptor of the overall SF structure of the scene. From this perspective, the visual composition of Typology C appears to be closer to natural-scene statistics than that of Typologies A and B.

Compared with the other typologies, Typology C combines greater visible sky exposure with a more articulated and fragmented street-level façade. Prior research suggests that greater sky exposure is associated with improved mood and reduced oppression in dense urban settings (Asgarzadeh et al., 2014; Chen et al., 2012; Xiang et al., 2021). A more articulated façade with richer visual detail may also be associated with greater retention of high-frequency information in the scene (Ellemberg et al., 2012; Ginsburg, 1986). In the present study, however, these visible features were not tested as independent determinants, but are understood as co-varying morphological attributes that may jointly shape the overall SF structure of the scene.

From the perspective of amplitude spectrum slope, Typology C exhibited the α value closest to 1, which is also closest to the statistical regularity commonly reported for natural scenes (Field, 1987). Because the human visual system is considered to be well adapted to this type of image structure, scenes whose α values approach 1 may be processed more fluently and experienced as more comfortable (Field, 1987; Oliva & Torralba, 2001; Penacchio & Wilkins, 2015).

Therefore, the comparatively lower physiological stress observed in Typology C is interpreted here as being associated with its overall visual-statistical configuration rather than with any single feature considered in isolation. Visible sky exposure and façade articulation may be attributes that jointly contribute to an α value closer to 1 and may be associated, under the tested conditions, with a lower stress response.

Cantilevered buildings and super high-rise podium-tower: higher relative physiological stress

In contrast to Typology C, Typologies A and B were associated with higher physiological stress. Typology

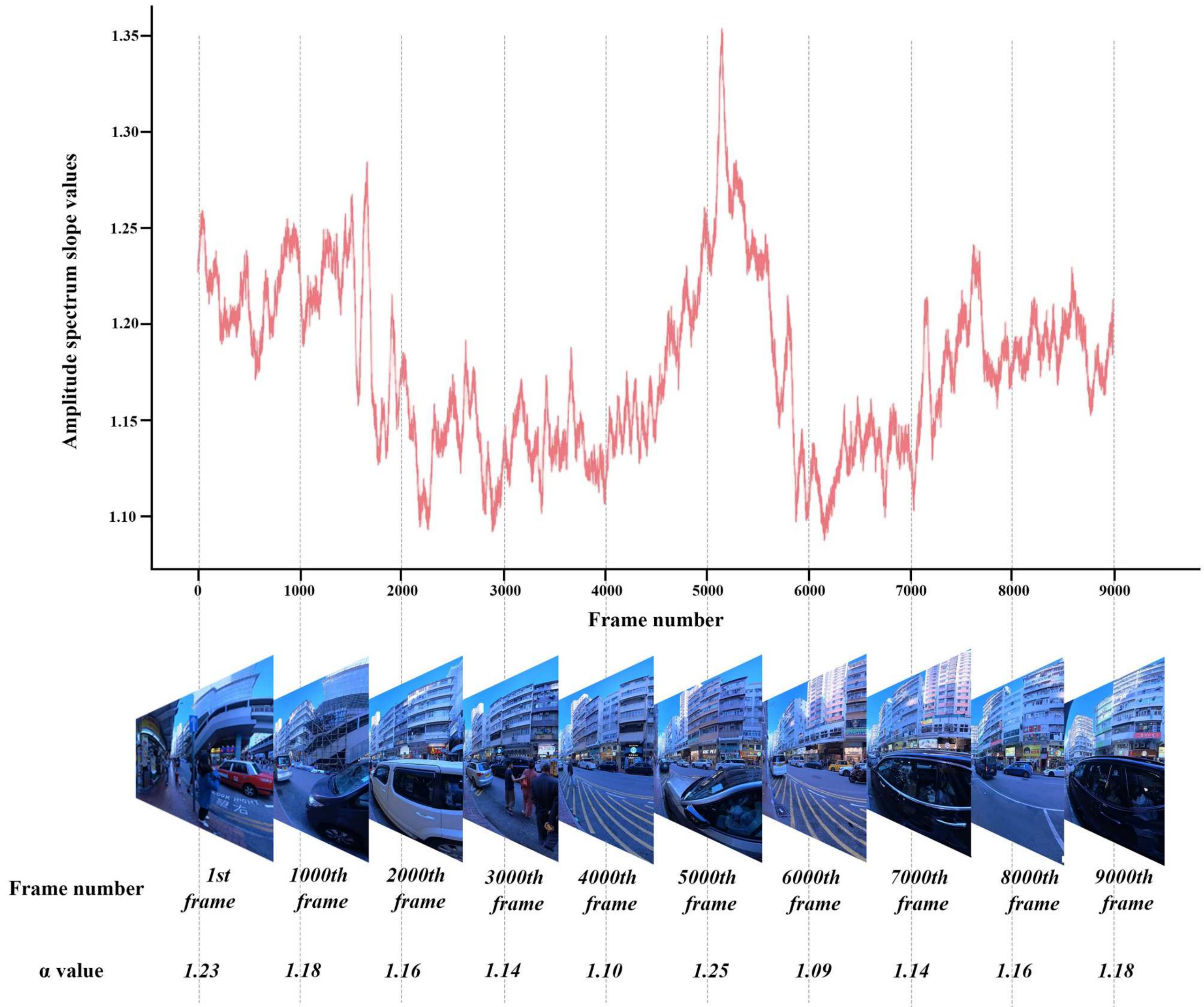

Figure 10. Variation of α values for Typology C over time; representative frames are shown at 998-frame intervals.

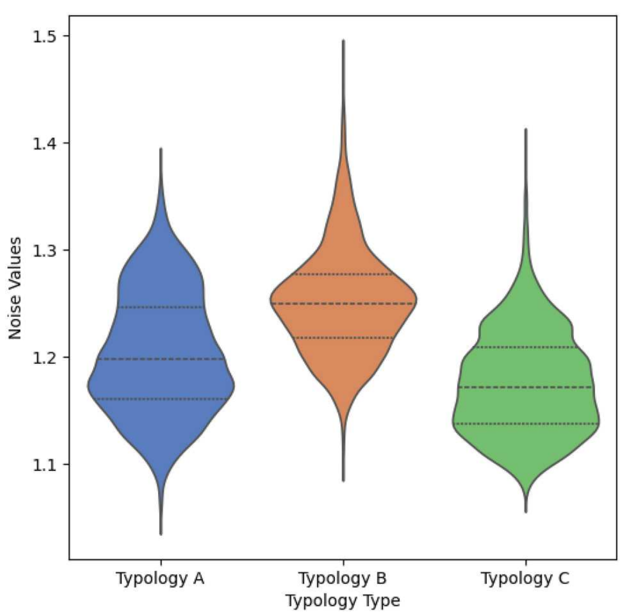

Figure 11. Distribution of α values for building typologies A, B, and C.

A showed a moderate α value (1.2037) but the lowest SDNN, indicating the highest stress response, whereas Typology B showed the highest α value (1.2514) and also higher stress than Typology C. Overall, these results suggest that typologies whose α values deviate further from 1 may be associated with less comfortable perceptual conditions (Field, 1987; Juricevic et al., 2010).

For Typology A, the dense commercial use at lower levels and the compact cantilevered built form may have contributed to a stronger sense of visual oppression. For Typology B, limited sky exposure and a cleaner, less fragmented façade are consistent with its higher α value,

Table 2. Summary of α and SDNN values for typologies.

	Indicates	Typology A	Typology B	Typology C
Average	α values	1.2037	1.2514	1.1758
	SDNN	48.23	49.60	54.39
Standard Deviation	α values	0.0566	0.0496	0.0479
	SDNN	13.05	12.12	12.92

Table 3. One-way ANOVA results for α values of images cropped at a vertical gaze angle of ± 45 degrees.

	Sum of squares	df	Mean square	F	Sig.
Between groups	26.331	2	13.166	4964.269	≤ 0.05
Within groups	71.598	26997	0.003		
Total	97.929	26999			

indicating a relative reduction in high-frequency information. Prior studies suggest that reduced sky exposure in dense urban settings can worsen emotional experience and intensify oppression (Asgarzadeh et al., 2014; Xiang et al., 2021), while environments with fewer detailed features tend to exhibit higher α values (Flitcroft et al., 2020). These observations support the view that different morphological attributes may jointly shape the scene-level SF structure, rather than acting as isolated determinants of stress.

Notably, although Typology B had a significantly higher α value than Typology A, no significant SDNN difference was observed between them. This suggests that the relationship between α and stress may not be strictly linear across all typologies. A possible explanation is that visual sensitivity to amplitude spectrum slope is strongest when α is closer to the natural value of approximately 1 and weakens as α deviates further from that range (Spehar et al., 2015). In this sense, the clearest contrast lies not between Typologies A and B, but between Typology C and the two typologies whose visual patterns departed further from $\alpha \approx 1$.

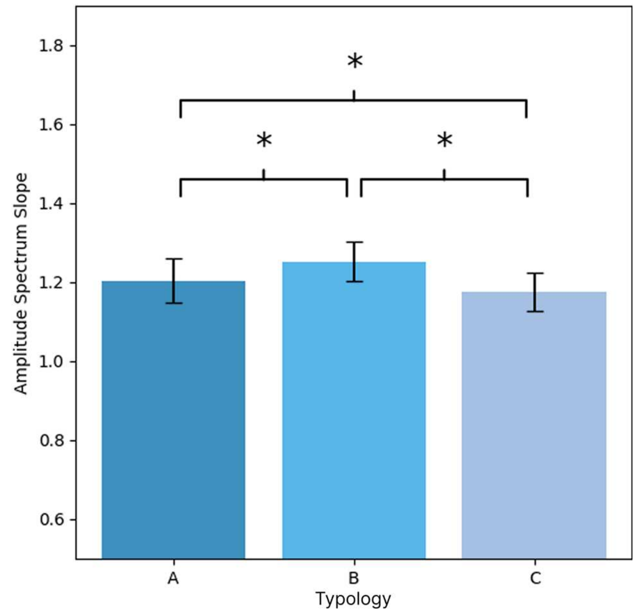

Figure 12. Mean and standard errors of α values for each experimental condition. *Statistical significance at 0.05.

Design implications and methodological contribution

This study investigated the association between building typology and relative physiological stress, interpreted through amplitude spectrum slope analysis. Under the tested conditions, building typologies with α values closer to 1 were associated with comparatively lower physiological stress. Rather than implying that α should be treated as a direct design target, this result highlights the potential value of considering the overall visual-statistical configuration of streetscapes in high-density urban environments.

From a design perspective, typology-related visual attributes, such as visible sky exposure, façade articulation, and overall scene complexity, may be relevant to physiological stress experience. However, these attributes were not independently manipulated in the present study and therefore should not be interpreted as isolated determinants. Instead, the findings support an integrated view in which building typology shapes scene-level SF structure, which is associated with relative differences in physiological stress.

Methodologically, this study combines image-based $1/f^{\alpha}$ analysis with physiological monitoring to provide a quantitative way of examining human–environment interaction. The results suggest that amplitude spectrum slope may serve as a useful descriptor of the visual structure of built environments, while future research may extend this framework by testing a wider range of urban typologies, incorporating more independently measured visual variables, and applying the method to other urban contexts, such as historic districts, streets

Table 5. Summary of Mean α value and SDNN values for each building typology.

Conditions	Mean α value	SDNN results	Rank (Mean α *value*/SDNN)[a]
Typology A	1.2037	48.23	2/3
Typology B	1.2514	49.60	3/2
Typology C	1.1758	54.39	1/1

[a]Mean α value and SDNN are listed from the highest to the lowest values.

Table 4. Post hoc test results of α values for images cropped at a vertical gaze angle of ± 45 degrees.

	Typology number	Typology number (j)	Mean difference (i-j)	Std. error	Sig.	Low bound	Upper bound
Bonferroni	Typology A	Typology B	0.0478*	0.0008	≤ 0.05	0.0459	0.0496
		Typology C	−0.0279*	0.0008	≤ 0.05	−0.0297	−0.0260
	Typology B	Typology C	−0.0756*	0.0008	≤ 0.05	−0.0775	−0.0738

with greater green infrastructure, or mixed natural–built settings.

Limitations and future study

One limitation of the present study is its reliance on controlled VR environments and standardized image crops, derived from pre-recorded video stimuli, which may not fully capture the complexity of real-world interactions with building typologies. In addition, the amplitude spectrum slope was calculated from standardized scene images rather than participant-specific visual views. Because autonomic responses may show temporal latency following visual stimuli, and because SDNN is a window-based HRV measure typically derived over several minutes (Shaffer et al., 2020; Shaffer & Ginsberg, 2017), the relationship between α and SDNN should be interpreted at the typology or condition level, rather than as a direct moment-to-moment correspondence between visual input and physiological response. In addition, specific visual attributes were not independently manipulated or quantified in the present study, and their individual contributions cannot be isolated from the current design.

A further limitation is that no pre-exposure physiological baseline was recorded. Accordingly, the physiological results should be interpreted as relative differences in SDNN across the three typology-specific conditions rather than as absolute changes from an initial resting state. This also means that potential initial-state and carryover effects across the sequential exposure phases cannot be fully excluded. In addition, this study does not account for subjective factors, such as personal preferences or prior experiences, which can significantly influence stress responses.

Although SDNN is widely used as a robust physiological indicator of stress, it may not fully encompass the multifaceted nature of stress, which can also involve emotional and behavioural dimensions that were not captured in this study. Moreover, the age range of participants in this study was relatively narrow, which limits the generalizability of the findings to broader populations.

Future research should adopt a more comprehensive approach by combining physiological, subjective, and behavioural indicators of stress. In particular, future studies could incorporate pre-exposure baseline measurements, self-reported stress ratings, and cognitive performance tests, as well as participant-specific gaze data, to clarify how moment-to-moment visual input relates to physiological stress. For questions involving finer-grained temporal coupling, future studies may also benefit from higher-temporal-resolution measures, such as Electroencephalography, together with participant-specific visual data. It would also be valuable to include participants from a wider age range and to examine how additional environmental factors such as greenery, lighting, noise, and social density, interact with scene-level SF structure to shape stress responses in urban environments. For example, greenery and expansive views may alleviate stress caused by high visual complexity and promote positive emotions (Xiang et al., 2021), while noise or overcrowding could intensify stress, even in simpler environments. These factors may either mitigate or intensify the physiological effects associated with different streetscape configurations. Understanding these interactions would help inform urban design strategies that combine various elements to enhance comfort and reduce stress in everyday settings.

Conclusion

This study investigated how building typology is associated with relative physiological stress by integrating amplitude spectrum slope analysis with immersive VR exposure and HRV measurement. The results showed that the building typology with an α value closest to 1, which is more consistent with natural-scene statistics, was associated with comparatively lower physiological stress under the tested conditions. Specifically, the podium-tower typology (Typology C) exhibited the lowest mean α value and the highest SDNN, indicating lower relative physiological stress than the other two typologies.

These results demonstrate the value of linking scene-level SF structure to stress-related physiological responses in the evaluation of urban streetscapes. Rather than reducing the effect to any single visual feature, the study highlights the importance of the overall visual-statistical configuration of building typologies in high-density environments. In this sense, the framework developed here extends earlier Fourier-based streetscape research by introducing a new way to connect image-based SF analysis with objective physiological evidence. This offers a useful methodological basis for future research and for evidence-informed urban design aimed at healthier and less stressful street environments.

Acknowledgements

We would like to deeply thank Jiaxin Zhu for her precious support with data collection, experiment setting, and framework, Junpai Chen for his support with data analysis and framework, and Jiakun Pei for his support with the manuscript visuals. We would also like to extend our thanks to all the participants who contributed to the study. During the preparation of this work, the authors used DeepSeek R1 to improve the readability and language of the article. After using this tool/service, the authors reviewed and edited the content as needed and take full responsibility for the content of the publication.

Author contributions

CRediT: **Mirna Zordan:** Conceptualization, Investigation, Methodology, Project administration, Resources, Supervision, Visualization, Writing – original draft, Writing – review & editing; **Petrus Jacobus Hermanus Maree:** Conceptualization, Formal analysis, Methodology, Software, Writing – review & editing; **Zixian Lei:** Data curation, Formal analysis, Software, Validation, Visualization, Writing – review & editing; **Tianze Xie:** Data curation, Software, Writing – review & editing; **Seungwoo Je:** Data curation, Formal analysis, Methodology, Validation, Writing – review & editing.

Disclosure statement

No potential conflict of interest was reported by the author(s).

Data availability statement

The data that support the findings of this study are available from the corresponding author, upon reasonable request (data available on request from the authors). The data includes sensitive biometric data that we are not able to make publicly available due to privacy concerns.

ORCID

Mirna Zordan http://orcid.org/0000-0002-8436-2898
Petrus Jacobus Hermanus Maree http://orcid.org/0009-0008-3870-2418
Zixian Lei http://orcid.org/0009-0003-8208-3291
Tianze Xie http://orcid.org/0009-0003-8884-6069
Seungwoo Je http://orcid.org/0000-0002-3968-7298

References

Acharya, U. R., Joseph, P. K., Kannathal, N., Lim, C. M., & Suri, J. S. (2006). Heart rate variability: A review. *Medical & Biological Engineering & Computing*, *44*(12), 1031–1051. https://doi.org/10.1007/s11517-006-0119-0

Asgarzadeh, M., Koga, T., Hirate, K., Farvid, M., & Lusk, A. (2014). Investigating oppressiveness and spaciousness in relation to building, trees, sky and ground surface: A study in Tokyo. *Landscape and Urban Planning*, *131*, 36–41. https://doi.org/10.1016/j.landurbplan.2014.07.011

Barbieri, R., Matten, E. C., Alabi, A. A., & Brown, E. N. (2005). A point-process model of human heartbeat intervals: New definitions of heart rate and heart rate variability. *American Journal of Physiology-Heart and Circulatory Physiology*, *288*(1), H424–H435. https://doi.org/10.1152/ajpheart.00482.2003

Baum, A., & Weiss, L. (1987). Social density and perceived control as mediators of crowding stress in high-density residential neighborhoods. *Journal of Personality and Social Psychology*, *52*(5), 899–906. https://doi.org/10.1037/0022-3514.52.5.899

Bex, P. J., & Makous, W. (2002). Spatial frequency, phase, and the contrast of natural images. *Journal of the Optical Society of America A*, *19*(6), 1096–1106. https://doi.org/10.1364/JOSAA.19.001096

Boubekri, M., Cheung, I. N., Reid, K. J., Wang, C. H., & Zee, P. C. (2014). Impact of windows and daylight exposure on overall health and sleep quality of office workers: A case-control pilot study. *Journal of Clinical Sleep Medicine*, *10*(6), 603–611. https://doi.org/10.5664/jcsm.3780

Buttazzoni, A., & Minaker, L. (2023). Exploring the relationships between specific urban design features and adolescent mental health: The case of imageability, enclosure, human scale, transparency, and complexity. *Landscape and Urban Planning*, *235*, 104736. https://doi.org/10.1016/j.landurbplan.2023.104736

Campbell, F. W., & Robson, J. G. (1968). Application of Fourier analysis to the visibility of gratings. *The Journal of Physiology*, *197*(3), 551–566. https://doi.org/10.1113/jphysiol.1968.sp008574

Cavalcante, A., Mansouri, A., Kacha, L., Barros, A. K., Takeuchi, Y., Matsumoto, N., & Ohnishi, N. (2014). Measuring streetscape complexity based on the statistics of local contrast and spatial frequency. *PLoS One*, *9*(2), e87097. https://doi.org/10.1371/journal.pone.0087097

Celikors, E., & Wells, N. M. (2022). Are low-level visual features of scenes associated with perceived restorative qualities? *Journal of Environmental Psychology*, *81*, 101800. https://doi.org/10.1016/j.jenvp.2022.101800

Chen, L., Ng, E., An, X., Ren, C., Lee, M., Wang, U., & He, Z. (2012). Sky view factor analysis of street canyons and its implications for daytime intra-urban air temperature differentials in high-rise, high-density urban areas of Hong Kong: A GIS-based simulation approach. *International Journal of Climatology*, *32*(1), 121–136. https://doi.org/10.1002/joc.2243

de Groot, J. H., Kirk, P. A., & Gottfried, J. A. (2021). Titrating the smell of fear: Initial evidence for dose-invariant behavioral, physiological, and neural responses. *Psychological Science*, *32*(4), 558–572. doi:10.1177/0956797620970548

Ellemberg, D., Hansen, B. C., & Johnson, A. (2012). The developing visual system is not optimally sensitive to the spatial statistics of natural images. *Vision Research*, *67*, 1–7. https://doi.org/10.1016/j.visres.2012.06.018

Epstein, R. A., Higgins, J. S., Jablonski, K., & Feiler, A. M. (2007). Visual scene processing in familiar and unfamiliar environments. *Journal of Neurophysiology*, *97*(5), 3670–3683. https://doi.org/10.1152/jn.00003.2007

Evans, G. W., Wells, N. M., & Moch, A. (2003). Housing and mental health: A review of the evidence and a methodological and conceptual critique. *Journal of Social Issues*, *59*(3), 475–500. https://doi.org/10.1111/1540-4560.00074

Ewing, R. (2013). *Eight qualities of pedestrian- and transit-oriented design*. Urban Land. https://urbanland.uli.org/infrastructure-transit/eight-qualities-of-pedestrian-and-transit-oriented-design.

Fernandez, D., & Wilkins, A. J. (2008). Uncomfortable images in art and nature. *Perception*, *37*(7), 1098–1113. https://doi.org/10.1068/p5814

Field, D. J. (1987). Relations between the statistics of natural images and the response properties of cortical cells. *Journal of the Optical Society of America A*, *4*(12), 2379–2394. https://doi.org/10.1364/JOSAA.4.002379

Flitcroft, D. I., Harb, E. N., & Wildsoet, C. F. (2020). The spatial frequency content of urban and indoor environments as a potential risk factor for myopia development. *Investigative Opthalmology & Visual Science*, *61*(*11*), 42. https://doi.org/10.1167/iovs.61.11.42

Gaertner, R. J., Kossmann, K. E., Benz, A. B., Bentele, U. U., Meier, M., Denk, B. F., Klink, E. S. C., Dimitroff, S. J., & Pruessner, J. C. (2023). Relaxing effects of virtual environments on the autonomic nervous system indicated by heart rate variability: A systematic review. *Journal of Environmental Psychology*, *88*, 102035. https://doi.org/10.1016/j.jenvp.2023.102035

Gao, X., Geng, Y., Spengler, J. D., Long, J., Liu, N., Luo, Z., Kalantari, S., & Zhuang, W. (2025). Evaluating the impact of spatial openness on stress recovery: A virtual reality experiment study with psychological and physiological measurements. *Building and Environment*, *269*, 112434. https://doi.org/10.1016/j.buildenv.2024.112434

Ginsburg, A. P. (1971). *Psychological correlates of a model of the human visual system* (Report No. GEEE71S2).

Ginsburg, A. P. (1986). Spatial filtering and visual form perception. In K. R. Boff, L. Kaufman, & J. P. Thomas (Eds.), *Handbook of perception and human performance* (Vol. 2, pp. 34-1–34-41). Cognitive Processes and Performance. Wiley.

Harper, S., Michailidou, E., & Stevens, R. (2009). Toward a definition of visual complexity as an implicit measure of cognitive load. *ACM Transactions on Applied Perception*, *6*(2), 1–18. https://doi.org/10.1145/1498700.1498704

Hartig, T., Mitchell, R., de Vries, S., & Frumkin, H. (2014). Nature and health. *Annual Review of Public Health*, *35*(1), 207–228. https://doi.org/10.1146/annurev-publhealth-032013-182443

Hashemi Kashani, S. M., Pazhouhanfar, M., & van Oel, C. J. (2023). Role of physical attributes of preferred building facades on perceived visual complexity: A discrete choice experiment. *Environment, Development and Sustainability*, *26*(5), 13515–13534. https://doi.org/10.1007/s10668-023-02980-0

Isherwood, Z. J., Schira, M. M., & Spehar, B. (2017). The tuning of human visual cortex to variations in the 1/fα amplitude spectra and fractal properties of synthetic noise images. *NeuroImage*, *146*, 642–657. https://doi.org/10.1016/j.neuroimage.2016.10.013

Jacquin, A. E. (1992). Image coding based on a fractal theory of iterated contractive image transformations. *IEEE Transactions on Image Processing*, *1*(1), 18–30. https://doi.org/10.1109/83.128028

Juricevic, I., Land, L., Wilkins, A., & Webster, M. A. (2010). Visual discomfort and natural image statistics. *Perception*, *39*(7), 884–899. https://doi.org/10.1068/p6656

Kaplan, S., Kaplan, R., & Wendt, J. S. (1972). Rated preference and complexity for natural and urban visual material. *Perception & Psychophysics*, *12*(4), 354–356. https://doi.org/10.3758/BF03207221

Kim, H. G., Cheon, E. J., Bai, D. S., Lee, Y. H., & Koo, B. H. (2018). Stress and heart rate variability: A meta-analysis and review of the literature. *Psychiatry Investigation*, *15*(3), 235–245. https://doi.org/10.30773/pi.2017.08.17

Kozaki, T., Miura, N., Takahashi, M., & Yasukouchi, A. (2012). Effect of reduced illumination on insomnia in office workers. *Journal of Occupational Health*, *54*(4), 331–335. https://doi.org/10.1539/joh.12-0049-FS

Lau, S. S. (2011). Physical environment of tall residential buildings: The case of Hong Kong. In B. Yuen, & A. G. O. Yeh (Eds.), *High-Rise living in Asian cities* (pp. 25–47). Springer.

Lau, S. S., & Zhang, Q. (2015). Genesis of a vertical city in Hong Kong. *International Journal of High-Rise Buildings*, *4*(2), 117–125. https://doi.org/10.21022/IJHRB.2015.4.2.117

Lenzholzer, S., & de Vries, S. (2020). Exploring outdoor thermal perception: A revised model. *International Journal of Biometeorology*, *64*(2), 293–300. https://doi.org/10.1007/s00484-019-01777-z

Liang, X., Chang, J. H., Gao, S., Zhao, T., & Biljecki, F. (2024). Evaluating human perception of building exteriors using street view imagery. *Building and Environment*, *263*, 111875. https://doi.org/10.1016/j.buildenv.2024.111875

Liu, J., Deng, G. H., Zhang, J., Wang, Y., Xia, X. Y., Luo, X. M., Liu, H., Zhang, X. Y., & Jiang, Y. (2015). The effect of chronic stress on anti-angiogenesis of sunitinib in colorectal cancer models. *Psychoneuroendocrinology*, *52*, 143–152. https://doi.org/10.1016/j.psyneuen.2014.11.006

Ma, L., Zhang, H., & Lu, M. (2020). Building's fractal dimension trend and its application in visual complexity map. *Building and Environment*, *178*, 106925. https://doi.org/10.1016/j.buildenv.2020.106925

Matsumoto, N., & Seta, S. (1999). The functional relations between anticipation and the space shape of curved streets. *Journal of Architecture and Planning (Transactions of AIJ)*, *64*(526), 153–158. https://doi.org/10.3130/aija.64.153_6

Oliva, A., Mack, M. L., Shrestha, M., & Peeper, A. (2004). Identifying the perceptual dimensions of visual complexity of scenes. *Proceedings of the Annual Meeting of the Cognitive Science Society*, *26*(26), 1041–1046.

Oliva, A., & Torralba, A. (2001). Modeling the shape of the scene: A holistic representation of the spatial envelope. *International Journal of Computer Vision*, *42*(3), 145–175. https://doi.org/10.1023/A:1011139631724

Penacchio, O., & Wilkins, A. J. (2015). Visual discomfort and the spatial distribution of Fourier energy. *Vision Research*, *108*, 1–7. https://doi.org/10.1016/j.visres.2014.12.013

Persiani, S. G., Kobas, B., Koth, S. C., & Auer, T. (2021). Biometric data as real-time measure of physiological reactions to environmental stimuli in the built environment. *Energies*, *14*(1), 232. https://doi.org/10.3390/en14010232

Rigau, J., Feixas, M., & Sbert, M. (2005, May). An information-theoretic framework for image complexity. *In Proceedings of the First Eurographics Conference on Computational Aesthetics in Graphics, Visualization and Imaging*, 177–184. https://doi.org/10.2312/COMPAESTH/COMPAESTH05/177-184

Scannell, L., & Gifford, R. (2017). The experienced psychological benefits of place attachment. *Journal of Environmental Psychology*, *51*, 256–269. https://doi.org/10.1016/j.jenvp.2017.04.001

Seta, S., Matsumoto, N., Aono, F., Kohno, T., & Musya, T. (2002). The influence of the street trees and the buildings with the fluctuation theory upon disorder, regularity and attraction of the streetscapes: Studies of disorder and regularity in the central business district Part 3. *Journal of Architecture and Planning (Transactions of AIJ)*, *67*(561), 181–188. https://doi.org/10.3130/aija.67.181_4

Seta, S., Matsumoto, N., & Tanabe, J. (2003). A study on usefulness of Fourier transform method for evaluating streetscapes: Studies on disorder and regularity in the central business district Part 4. *Journal of Architecture and Planning (Transactions of AIJ)*, *68*(569), 85–92. https://doi.org/10.3130/aija.68.85_4

Shaffer, F., & Ginsberg, J. P. (2017). An overview of heart rate variability metrics and norms. *Frontiers in Public Health*, *5*, 258. https://doi.org/10.3389/fpubh.2017.00258

Shaffer, F., Meehan, Z. M., & Zerr, C. L. (2020). A critical review of ultra-short-term heart rate variability norms research. *Frontiers in Neuroscience*, *14*, 594880. https://doi.org/10.3389/fnins.2020.594880

Snodgrass, J. G., & Vanderwart, M. (1980). A standardized set of 260 pictures: Norms for name agreement, image agreement, familiarity, and visual complexity. *Journal of Experimental Psychology: Human Learning and Memory*, *6*(2), 174–215. https://doi.org/10.1037/0278-7393.6.2.174

Spehar, B., Wong, S., van de Klundert, S., Lui, J., Clifford, C. W., & Taylor, R. P. (2015). Beauty and the beholder: The role of visual sensitivity in visual preference. *Frontiers in Human Neuroscience*, *9*, 514. https://doi.org/10.3389/fnhum.2015.00514

St-Jean, P., Clark, O. G., & Jemtrud, M. (2022). A review of the effects of architectural stimuli on human psychology and physiology. *Building and Environment*, *219*, 109182. https://doi.org/10.1016/j.buildenv.2022.109182

Tarvainen, M. P., Niskanen, J. P., Lipponen, J. A., Ranta-Aho, P. O., & Karjalainen, P. A. (2014). Kubios HRV: Heart rate variability analysis software. *Computer Methods and Programs in Biomedicine*, *113*(1), 210–220. https://doi.org/10.1016/j.cmpb.2013.07.024

Thayer, J. F., Hansen, A. L., & Johnsen, B. H. (2010). The non-invasive assessment of autonomic influences on the heart using impedance cardiography and heart rate variability. In A. Steptoe (Ed.), *Handbook of behavioral medicine: Methods and applications* (pp. 723–740). Springer.

Tuch, A. N., Bargas-Avila, J. A., Opwis, K., & Wilhelm, F. H. (2009). Visual complexity of websites: Effects on users' experience, physiology, performance, and memory. *International Journal of Human-Computer Studies*, *67*(9), 703–715. https://doi.org/10.1016/j.ijhcs.2009.04.003

Ulrich, R. S. (1991). Effects of interior design on wellness: Theory and recent scientific research. *Journal of Health Care Interior Design*, *3*, 97–109.

van Ast, V. A., Klumpers, F., Grasman, R. P., Krypotos, A. M., & Roelofs, K. (2022). Postural freezing relates to startle potentiation in a human fear-conditioning paradigm. *Psychophysiology*, *59*(4), e13983. https://doi.org/10.1111/psyp.13983

Vigo, D. E., Siri, L. N., & Cardinali, D. P. (2019). Heart rate variability: A tool to explore autonomic nervous system activity in health and disease. In P. Á. Gargiulo & H. L. Mesones Arroyo (Eds.), *Psychiatry and neuroscience update: From translational research to a humanistic approach—volume III* (pp. 113–126). Springer.

Wilkins, A. J. (2016). A physiological basis for visual discomfort: Application in lighting design. *Lighting Research & Technology*, *48*(1), 44–54. https://doi.org/10.1177/1477153515612526

Xiang, L., Cai, M., Ren, C., & Ng, E. (2021). Modeling pedestrian emotion in high-density cities using visual exposure and machine learning: Tracking real-time physiology and psychology in Hong Kong. *Building and Environment*, *205*, 108273. https://doi.org/10.1016/j.buildenv.2021.108273

Yeom, S., Kim, H., & Hong, T. (2021). Psychological and physiological effects of a green wall on occupants: A cross-over study in virtual reality. *Building and Environment*, *204*, 108134. https://doi.org/10.1016/j.buildenv.2021.108134

Zordan, M., & Je, S. (2024). Brain-load, stress levels, and visual complexity: Digital tools for the detection of intangible human-environment interactions. *XRDS: Crossroads, The ACM Magazine for Students*, *30*(3), 14–19. https://doi.org/10.1145/3652617